Noninvasive Red Laser Intervention before Radiotherapy of Triple-negative Breast Cancer in a Murine Model

Authors: Silva, Camila R., Pereira, Saulo T., Silva, Daniela F.T., De Pretto, Lucas R., Freitas, Anderson Z., et al.

Source: Radiation Research, 200(4) : 366-373

Published By: Radiation Research Society

URL: https://doi.org/10.1667/RADE-23-00050.1

RADIATION RESEARCH **200**, 366–373 (2023)
0033-7587/23 $15.00

DOI: 10.1667/RADE-23-00050.1

Noninvasive Red Laser Intervention before Radiotherapy of Triple-negative Breast Cancer in a Murine Model

Camila R. Silva,[a] Saulo T. Pereira,[a] Daniela F.T. Silva,[a] Lucas R. De Pretto,[a] Anderson Z. Freitas,[a] Carlos A. Zeituni,[b] Maria E.C.M. Rostelato,[b] Martha S. Ribeiro[a,1]

[a] Center for Lasers and Applications; [b] Radiation Technology Center, Nuclear and Energy Research Institute (IPEN-CNEN), São Paulo, SP, Brazil

Silva CR, Pereira ST, Silva DFT, De Pretto LR, Freitas AZ, Zeituni CA, Rostelato MECM, Ribeiro MS. Noninvasive Red Laser Intervention before Radiotherapy of Triple-Negative Breast Cancer in a Murine Model. Radiat Res. 200, 366–373 (2023).

Radiotherapy is a well-established cancer treatment; it is estimated that approximately 52% of oncology patients will require this treatment modality at least once. However, some tumors, such as triple-negative breast cancer (TNBC), may present as radioresistant and thus require high doses of ionizing radiation and a prolonged period of treatment, which may result in more severe side effects. Moreover, such tumors show a high incidence of metastases and decreased survival expectancy of the patient. Thus, new strategies for radiosensitizing TNBC are urgently needed. Red light therapy, photobiomodulation, has been used in clinical practice to mitigate the adverse side effects usually associated with radiotherapy. However, no studies have explored its use as a radiosensitizer of TNBC. Here, we used TNBC-bearing mice as a radioresistant cancer model. Red light treatment was applied in three different protocols before a high dose of radiation (60 Gy split in 4 fractions) was administered. We evaluated tumor growth, mouse clinical signs, total blood cell counts, lung metastasis, survival, and levels of glutathione in the blood. Our data showed that the highest laser dose in combination with radiation arrested tumor progression, likely due to inhibition of GSH synthesis. In addition, red light treatment before each fraction of radiation, regardless of the light dose, improved the health status of the animals, prevented anemia, reduced metastases, and improved survival. Collectively, these results indicate that red light treatment in combination with radiation could prove useful in the treatment of TNBC.

INTRODUCTION

Radiotherapy plays a pivotal role in the treatment of a variety of solid tumors, such as breast cancer (*1*). It is cost-effective as a single modality treatment, accounting for 5% of the total cost of cancer care. It has estimated that 52% of patients with cancer will receive radiation at some point during their treatment, either for curative or palliative purposes (*2*). Ionizing radiation used in radiation treatment induces cancer cells to die mainly by inducing DNA damage (*3*).

There is no standard radiation therapy protocol for all cancers, though it is often determined according to the type of cancer, stage, grade, and whether radiation is applied as a single or adjuvant treatment (*4–6*). For example, the European Society for Radiotherapy and Oncology Advisory in Radiation Oncology defined parameters of a moderate hypofractionation protocol (40–56 Gy in 15 or 16 fractions over 3 weeks) for treatment of the whole breast regardless of the age at breast cancer diagnosis, pathological tumor stage and breast cancer biology (*7*). Nonetheless, there are still challenges in radiotherapy to be overcome, such as minimizing the damage to normal cells/tissue surrounding the tumor and importantly, tumor radioresistance (*8*).

Radioresistant tumors generally are not responsive to other conventional cancer treatments and require high doses of radiation and a prolonged period of treatment; sometimes the treatments are only palliative, to provide quality of life to patients (*9*). Currently, technical advancements have improved radiotherapy and individual protocols. Indeed, most patients receive a general fractionation regimen (hypofractionation or ultra-hypofractionation) to facilitate treatment adherence, which has often been a concern (*10*). However, adverse effects such as fatigue, radiodermatitis, and loss of body mass that might occur during or after treatment have a direct impact on the physical, mental, and social well-being of the patient (*11*).

Tumors in triple-negative breast cancer (TNBC) patients are typically characterized as radioresistant, and not responsive to conventional anticancer therapies. However, due to the scarce treatment alternatives, radiation therapy is still often offered as a possible treatment to arrest cancer progression, mainly after the mastectomy (*11*). In general, TNBC represents 15% to 20% of the 2 million cases per year of breast cancer. Additionally, its mortality rate is high (40% within 5 years post-diagnosis) (*13*, *14*). It is also highly metastatic; 46% of patients develop distant metastases, mainly in the lung, with a life expectancy of only 13.3 months (*15*).

[1] Corresponding author: Martha Simões Ribeiro; email: marthasr@usp.br.

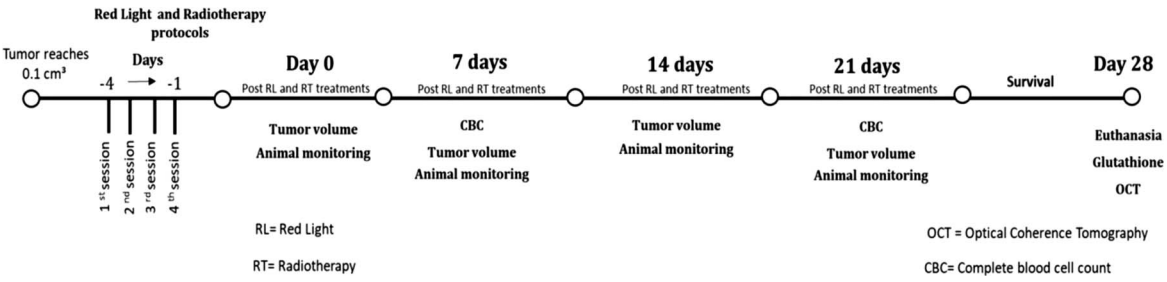

FIG. 1. Experimental study design.

The molecular mechanism of TNBC radioresistance remains unclear, though a recent study reported that radiation treatment increases levels of tripartite motif-containing protein 32 (TRIM 32), which is already upregulated in these cells (*16*). In this context, the search for radiosensitizers to reduce radioresistance is urgently required.

Photobiomodulation therapy (PBM), which employs non-ionizing radiation mostly in the range of red and near-infrared wavelengths from lasers or light-emitting diodes (LEDs), is a non-invasive approach that has been applied to restore, stimulate, and repair the damage caused by injury or diseases (*17*, *18*). Presently, PBM has been used to mitigate the side effects of breast cancer treatment, such as radiodermatitis and lymphedema (*19*, *20*). However, its use as a radiosensitizer for TNBC has not yet been explored. There are no specific radiosensitizers for TNBC, mainly due to the lack of an effective target for tumor suppression (*21*, *22*).

Previously, we showed that red light PBM applied after irradiation of TNBC tumor-bearing mice, regardless of the red light protocol, was able to arrest tumor growth, prevent side effects and hemolytic anemia, and reduce metastases (*23*). Here, we aimed to verify the ability of red light treatment to act as a radiosensitizer for TNBC. Using the same red light and radiation protocols, TNBC-bearing mice were exposed to red light treatment, and then animals received 4 fractions of 15 Gy (60 Gy). To evaluate the impact of the red light as a radiosensitizer, we also analyzed the tumor evolution, side effects, full blood count, lung metastasis by optical coherence tomography (OCT), and survival of treated mice. We also measured blood glutathione level, which is closely related to an animal's antioxidant defenses, to provide mechanistic insights.

MATERIALS AND METHODS

Breast cancer cells (4T1), used in established TNBC murine models, were cultured in RPMI 1640 medium (Sigma), supplemented with 10% fetal bovine serum (Sigma) at 37°C with 5% CO_2 in humidified air, and then, aliquoted at a concentration of 1×10^5 cells in 40 μL of the medium.

All experiments were performed according to the Ethics Committee on Animal Use of the Nuclear and Energy Research Institute (IPEN-CNEN). BALB/c female mice (n = 30) aged 6–8 weeks and with body mass of approximately 20 g were anesthetized with 2.5% isoflurane (Cristália, Brazil) by inhalation, trichotomized, and inoculated with 1×10^5 4T1 cells into the left mammary fat pad. All animals were monitored until the tumor volume reached 0.1 cm^3 (14 days post-inoculation) and randomized into 6 experimental groups on day 4 [tumor, radiation (IR), red light (RL) + IR, RL/IR, $RL_{37.5}$/IR and non-tumor bearing untreated animals (used to accumulate baseline values; 5 mice/group)] (Fig. 1).

Red light treatment was performed locally on tumors by using a laser (MMOptics Ltda, Brazil) ($\lambda = 660$ nm, an output power of 20 mW, spot area of 0.04 cm^2, power density of 500 mW cm^{-2}, exposure time of 37.5 and 150 s delivering energies of 1.5 and 6 J, and light doses of 37.5 and 150 Jcm^{-2}, respectively), in three different protocols (*23*): 1. single exposure 24 h before the first fraction of radiation with an energy density of 150 Jcm^{-2} (RL+IR group); 2. red light laser (150 Jcm^{-2}) applied immediately before each fraction (RL/IR group) or 3. red light laser (37.5 Jcm^{-2}) applied immediately before each fraction ($RL_{37.5}$/IR group). The laser tip was positioned at 90° on the tumor center to standardize the red light delivery.

Localized irradiations were carried out using a ^{60}Co panoramic irradiator (activity = 4.81 TBq) from Technology Radiation Center at IPEN. The distance between the breast and the source was kept constant at 10 cm and the dose rate dose was approximately 60 Gy h^{-1}. The total dose delivered to the breast tumor was 60 Gy split into 4 fractions of 15 Gy (one fraction per day). The mouse was inserted into a conical tube (50 mL) and shielded by a lead device, both of them with a hole in the breast region to allow irradiation of the tumor (*24*).

Tumor volume was measured daily by using digital calipers. We used the following equation to estimate tumor volume (*23*): V (cm^3) = $0.5 \times \text{length} \times \text{width}^2$.

Health Evaluation

Health status of mice was assessed weekly up to 21 days after the last fraction was administered. A trained and blinded veterinarian assigned scores for health status for each animal such as hypokinesia (0 = normal activity; 1 = reduced activity; 5 = inactive), piloerection (0 = no; 1 = yes), and hunching (0 = no; 1 = yes) ranging from 0 to 7. Higher scores indicate pain and distress, while lower scores denote better health status (*23*, *25*). The sum of the scores was computed for each experimental day.

Blood Examination

The levels of red blood cell (RBC), white blood cell (WBC), and platelet (PLT) counts were taken on days 7 and 21 after the last fraction by using a hematologic reader 2800 BCE VET (Mindray, China). Approximately 30 μL of blood was collected from the caudal vein and mixed with 1 μL of 10% sodium ethylenediaminetetraacetic acid (EDTA) to avoid blood coagulation.

Optical Coherence Tomography (OCT)

The animals were euthanized on day 28 using an excessive dose of anesthetics (30 mg kg^{-1} xylazine and 300 mg kg^{-1} ketamine). Blood samples were collected through subclavian vein puncture and centrifuged to obtain the plasma. Lungs were then aseptically removed for assessing metastatic nodules by OCT.

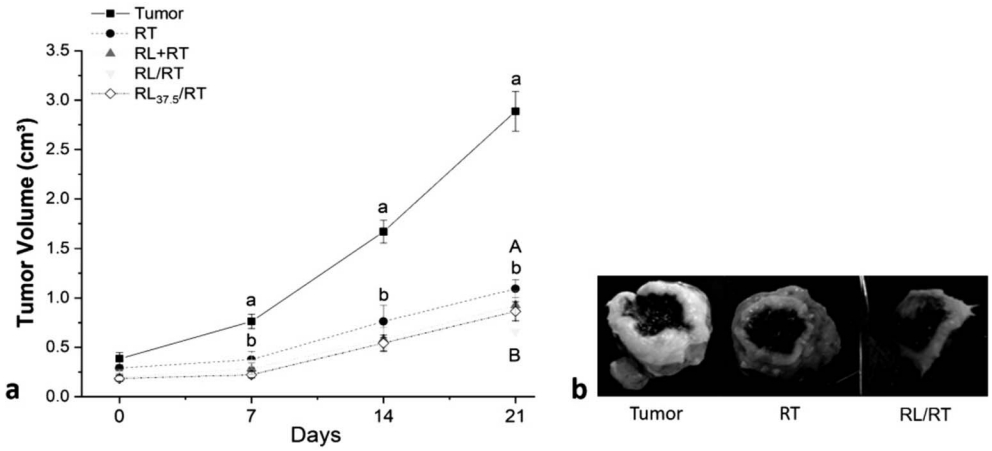

FIG. 2. Panel a: Tumor volume. Different lowercase letters (a, b) denote statistically significant differences between tumor control and irradiation (RT) groups at various times. Different uppercase letters (A, B) represent statistically significant differences between irradiation and red light/irradiation (RL/RT) groups. Data are presented as mean ± SEM with n = 5 animals/group. Panel b: Representative tumor images of the tumor control, RT, and RL/RT groups at the end of the experiment.

We used an OCT device with $\lambda = 1{,}300$ nm and an axial resolution of 10.6 μm (VEG220-Thorlabs®). Three-dimensional images of both sides of the lungs were constructed, and then the nodules were counted for each animal of each experimental group.

Glutathione Assay

Deproteinated samples, obtained from plasma, were used to determine individual values of reduced (GSH) and oxidized (GSSG) glutathione; samples were prepared using a glutathione quantification kit (Sigma) according to the manufacturer's protocol. The absorbance was measured using a spectrophotometer (SpectraMax M4, Molecular Devices) at $\lambda = 405$ nm and data are presented as GSH/GSSG ratio.

Statistical Analysis

The data distribution was verified by the Shapiro-Wilk test using the Origin Pro 2018 program. We used two-way repeated measures ANOVA for group comparisons of tumor volume and one-way ANOVA for the lung metastasis and glutathione assays. Fisher's test was used as a post-hoc test in both analyses. For animal health status, we performed the Kruskal-Wallis ANOVA and Mann-Whitney as post-tests. The log-rank test was used to assess the survival rate. Results are presented as means ± standard error of the mean (SEM) and as median ± interquartile range. Statistically significant differences were considered when $P < 0.05$.

RESULTS

Tumor Volume

We monitored tumor volume up to day 21 after irradiation because all animals were still alive (Fig. 2a). On day 0, which corresponds to 24 h after the treatment, the tumor control and irradiated groups showed similar tumor volumes (0.38 ± 0.06 cm^3 vs. 0.29 ± 0.07 cm^3). However, from day 7 to day 21, tumor volume in the tumor control group increased linearly, showing statistically significant differences compared to the irradiated group at all time points. On day 21, the tumor control group had a mean tumor volume 2.6-fold greater than the irradiated group (2.89 ± 0.20 cm^3 vs. 1.09 ± 0.09 cm^3, $P = 1.90 \times 10^{-8}$).

Conversely, when the red light was administered before irradiation, there was no significant change in tumor growth noted between groups until day 14, with the tumor volume reaching approximately 0.5 cm^3. Interestingly, red light treatment with irradiation significantly inhibited tumor growth on day 21; tumor volume was observed to be 40% lower (0.66 ± 0.11 cm^3) than the irradiation group (1.09 ± 0.09 cm^3, $P = 0.0051$). This inhibition was not noticed for the RL+IR (0.92 ± 0.15 cm^3) and $RL_{37.5}$/IR (0.86 ± 0.10 cm^3) groups. Figure 2b shows representative images of the tumor controls, irradiation and irradiation/red light groups at the end of the experimental period. It is worth noting that the tumor growth curve for each animal within a group was similar.

Health Status

Figure 3 shows the health status of the mice over the period of observation. We observed that exposure to radiation significantly induced pain and distress in mice on day 0, while the tumor control group did not. From the day 7 to day 21, no statistically significant differences were detected between the control and irradiation groups. In general, the most recurrent clinical symptoms for these groups were piloerection and hypokinesia. However, on day 21, three animals from the tumor control group showed complete inactivity.

Conversely, all red light groups maintained better health status than the irradiated group on days 0 and 7. Lower health scores were only recorded for the RL/IR and $RL_{37.5}$/IR groups on day 21. On the day 21 post-treatment, mice in the RL+IR group presented with hunched posture similar to the IR group, and one mouse was inactive.

Blood Measurements

We evaluated the blood at 2 time points: 7 and 21 days post-treatment (*20*). Reference values were obtained from

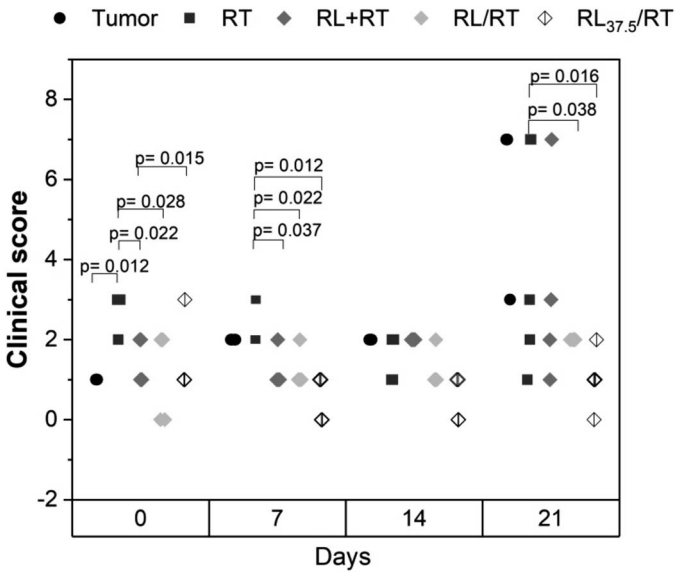

FIG. 3. Clinical monitoring and their respective health scores until day 21 post-treatment for all experimental groups. Each symbol represents an animal in each experimental group at the indicated time (n = 5 animals/group). Some symbols overlap since some animals within a group presented with the same score. Statistically significant differences were considered when $P < 0.05$.

healthy mice (n = 5), which were monitored and handled similarly over the experimental period.

On day 7, the tumor control group ($10.13 \pm 0.61 \times 10^{12}$ L^{-1}) exhibited RBC values within the reference interval ($10.02–12.55 \times 10^{12}$ L^{-1}) while the irradiated group was below reference levels ($8.81 \pm 0.17 \times 10^{12}$ L^{-1}) (Fig. 4a). On day 21, however, we observed a reduction of 4% and 10% in the RBC levels, respectively, compared to day 7.

The groups exposed to red light showed levels below the reference range on day 7. On the day 21, these groups had an increase in the RBC levels compared to day 7, even though only the RL/IR group ($9.70 \pm 0.43 \times 10^{12}$ L^{-1}) maintained levels close to the reference values.

The hemoglobin levels (Fig. 4b) for tumor control and irradiation groups were similar on days 7 and 21, and within the reference range (11.80–18.80 gdL^{-1}). In contrast, the RBC levels for the groups IR+RL and $RL_{37.5}$/IR were below reference values on day 7, but increased about 1.28-fold on day 21 to approximate the reference range values. The RL/IR group maintained hemoglobin levels within reference the reference range at both time points.

Regarding the hematocrit percentage (Fig. 4b), the tumor control group was within reference values on day 7 (52.40–68.70%), even though on day 21 a lower percentage was observed. On the other hand, IR and RL+IR groups exhibited values below reference levels on both days. Hematocrit percentages for RL/IR and $RL_{37.5}$/IR groups increased to reach the reference range on day 21.

Figure 4c shows PLT counts for all experimental groups. The values for the tumor control group are within the reference interval [$321.0 – 1,837.0 \times 10^9$ L^{-1}] for both time points. However, the irradition group showed low PLT levels on day 7 ($108.40 \pm 28.62 \times 10^9$ L^{-1}), even though PLT counts were comparable to the tumor control group on day 21 ($805.20 \pm 225.02 \times 10^9$ L^{-1} vs. $886.75 \pm 151.35 \times 10^9$ L^{-1}, respectively). Similar to the irradiation group, all groups treated with

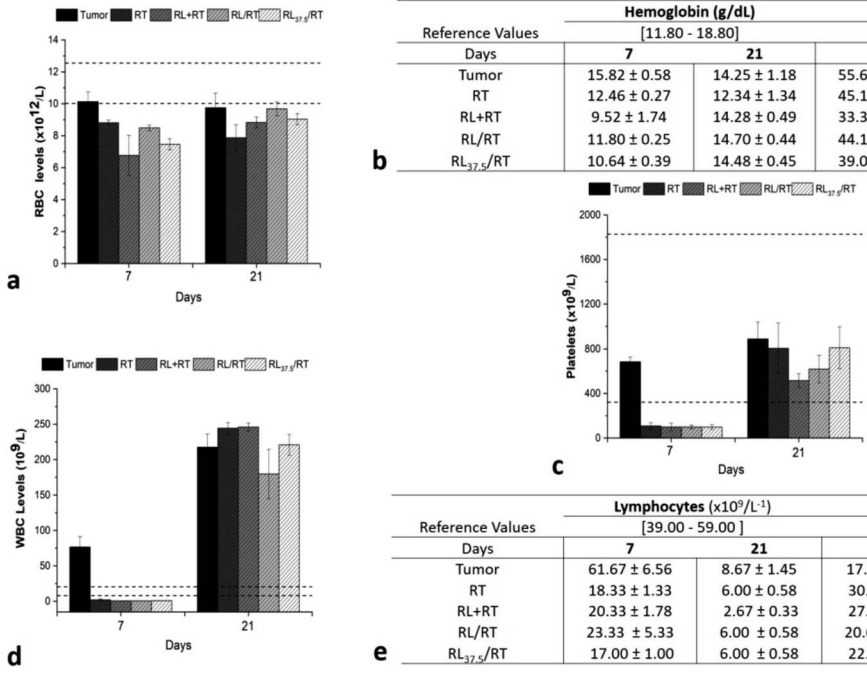

b

Reference Values	Hemoglobin (g/dL) [11.80 - 18.80]		Hematocrit (%) [52.40 - 68.70]	
Days	7	21	7	21
Tumor	15.82 ± 0.58	14.25 ± 1.18	55.60 ± 2.36	47.07 ± 3.24
RT	12.46 ± 0.27	12.34 ± 1.34	45.18 ± 0.91	39.00 ± 4.48
RL+RT	9.52 ± 1.74	14.28 ± 0.49	33.34 ± 6.21	43.44 ± 3.26
RL/RT	11.80 ± 0.25	14.70 ± 0.44	44.10 ± 1.14	49.72 ± 2.44
$RL_{37.5}$/RT	10.64 ± 0.39	14.48 ± 0.45	39.00 ± 2.40	49.84 ± 2.89

e

Reference Values	Lymphocytes (x10^9/L^{-1}) [39.00 - 59.00]		Neutrophils (x10^9/L^{-1}) [8.00 - 20.00]	
Days	7	21	7	21
Tumor	61.67 ± 6.56	8.67 ± 1.45	17.00 ± 5.13	55.00 ± 3.71
RT	18.33 ± 1.33	6.00 ± 0.58	30.67 ± 6.36	49.33 ± 4.91
RL+RT	20.33 ± 1.78	2.67 ± 0.33	27.33 ± 5.33	53.67 ± 5.46
RL/RT	23.33 ± 5.33	6.00 ± 0.58	20.67 ± 4.37	34.00 ± 1.53
$RL_{37.5}$/RT	17.00 ± 1.00	6.00 ± 0.58	22.67 ± 3.71	51.67 ± 11.33

FIG. 4. Blood counts for all experimental groups on days 7 and 21 post-treatment. Panel a: RBC levels; panel b: WBC levels; panel c: PLT levels; panel d: RBC indices; panel e: WBC indices. Data are presented as mean ± SEM and the lines represent the reference interval (minimum and maximum) for each experimental group with n = 5 animals/group.

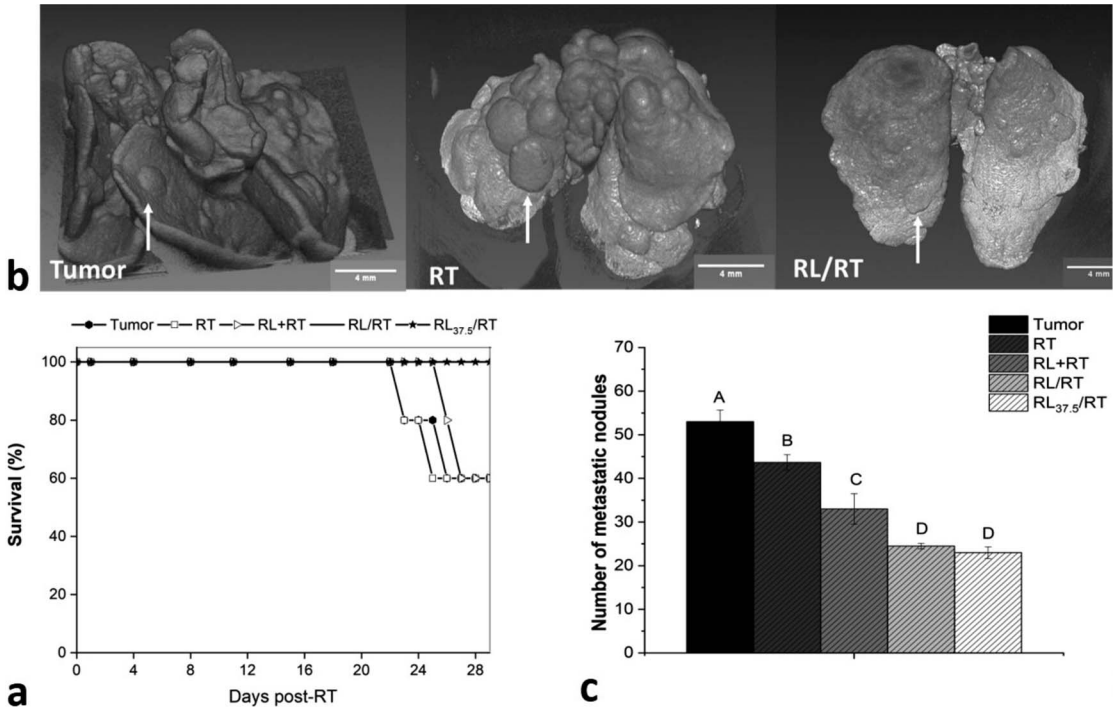

FIG. 5. Panel a: Survival through 28 days for each experimental group; Panel b: Representative 3D images of OCT of the mouse lungs for tumor control, irradiation (RT) and red light/irradiation (RL/RT) groups. The arrows point to metastatic nodules. Bar = 4 mm; and panel c: Number of lung metastatic nodules identified by 3D images of OCT. Different capital letters represent statistically significant differences among groups. Data are presented as mean ± SEM with 3 animals/group. The three mice in the RL/RT group were randomly selected while there were 3 living animals in the other groups.

red light exhibited low PLT levels on day 7, but reached reference levels 14 days later.

WBC counts for the tumor control group were above the reference range (7.90 – 20.50 × 10^9 L^{-1}), regardless of the time analyzed (Fig. 4d). The irradiation group, however, showed the opposite behavior on day 7 (2.18 ± 1.01 × 10^9 L^{-1}). On day 21, WBC levels were 12 times above the reference range (244.30 ± 8.23 × 10^9 L^{-1}). Red light groups, regardless of the protocol, showed data very similar to the irradiation group.

Except for the tumor control group, in which lymphocyte levels were within the reference range on day 7 but decreased on day 21, all groups showed lymphocyte counts outside of the normal range on days 7 and 21 (Fig. 4e). Indeed, irradiation and red light groups exhibited low lymphocyte counts on day 7 that further diminished by day 21.

Neutrophils, on the other hand, increased over time for all groups regardless of the protocol, showing levels out of the normal range on day 21. However, the irradiation group showed high levels of neutrophils on day 7.

Survival, Metastases and Glutathione Levels

The percentage of mice surviving was evaluated on day 28 post-treatment (Fig. 5a), after which they were euthanized; though we noted that mice started to die on day 23, 60% of mice in the tumor control and irradiation groups survived. The group with a single red light treatment had the same percentage of surviving mice as the irradiation group, but mice began to die on day 26. On the other hand, when red light treatment was administered with each radiation fraction (RL/IR and RL37.5/IR protocols), the percentage of mice surviving was 100%.

After euthanasia, the lungs were removed for evaluation by OCT. Three-dimensional images were constructed and the number of metastases was counted for each animal according to the experimental group (Fig. 5b). We observed that the number of metastatic nodules (Fig. 5c) was similar between the tumor controls (53.00 ± 2.65) and IR (43.67 ± 1.76, P = 0.007) groups. The RL+IR group (33.00 ± 3.51, P = 0.03), the RL/IR (23.00 ± 1.34, P = 2.90 × 10^{-5}), and $RL_{37.5}$/IR (25.00 ± 2.61, P = 1.64 × 10^{-5}) groups had a significantly lower number of metastatic nodules compared to the irradiation group.

To gain some insights into the role of red light treatment in radiosensitizing the tumor, we evaluated glutathione levels (Fig. 6). The irradiation group showed a GSH/GSSG ratio higher than the tumor control group (34.5 ± 6.75 vs. 12.6 ± 1.06, respectively), but not significantly different statistically. Interestingly, the RL/IR group exhibited GSH/GSSG levels significantly lower than irradiation groups (0.95 ± 0.22, P = 2.08 × 10^{-6}) but similar to the ratio of healthy mice (1.41 ± 0.07).

DISCUSSION

Our results showed that the highest laser dose (150 Jcm^{-2}) administered before each radiation fraction sensitized the

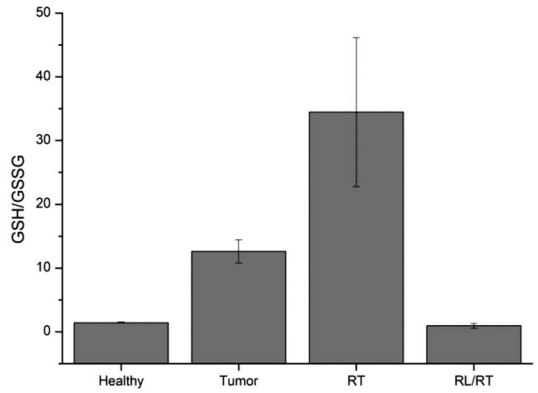

FIG. 6. GSH/GSSG ratios were measured using the blood from healthy mice, tumor control, irradiation (IR) and red light/irradiation (RL/RT) groups. Different capital letters represent statistically significant differences between groups. Data are presented as mean ± SEM with n = 3 animals/group.

radioresistant tumor; sensitization was probably due to impairment of the synthesis of the GSH. In addition, red light treatment with each dose of radiation, regardless of the light dose, resulted in improved health status, longer survival and a higher survival percentage, and a lower number of lung metastases.

In our studies, we used a 60 Gy dose, 4 fractions of 15 Gy, which was based on the European Society for Radiotherapy and Oncology Advisory in Radiation Oncology Practice guidelines for whole breast irradiation and adapted to our animal model (*7*). This treatment significantly arrested tumor progression, even though it worsened the health status of mice immediately after irradiation. These data confirm that high doses of radiation are required to control TNBC, but impact the general health status of the mice (*11*). On the other hand, our data demonstrate that red light treatment before each fraction of radiation, regardless of the light dose, did not significantly adversely affect health status, suggesting that red light treatment could prevent the side effects caused by radiation the clinic.

The blood count is an important laboratory test used to monitor a patient's response to cancer treatment. We observed a decrease in the RBC, WBC, and PTL counts for all groups irradiated on day 7. This result can be explained by the anatomical region of the tumor, the high dose of radiation, and its tissue penetration depth, which may cause temporary bone marrow suppression (*26*). Indeed, the normal levels of PTLs on day 21 indicate a bone marrow recovery.

At the same time point, however, IR and RL+IR groups still showed lower levels of RBC counts and hemocrit percentage. We also noticed that the tumor control group exhibited a low hematocrit percentage. These data are characteristic of an anemic condition and were not surprising since the TNBC model used in our study leads to the development of acute anemia during its progression (*27*). Additionally, it has been reported that anemia was observed in 75% of cancer patients after radiation therapy, and its severity and maintenance were related to the radiation dose (*28*). Remarkably, the highest dose of red light before each radiation fraction seemed to prevent anemia, since we noticed levels of RBCs and hemoglobin within the reference range on day 21.

WBCs are defense cells and their counts can be predictive of cancer remission or progression over time (*29*). On day 21, all groups exhibited an increase in WBC levels as expected (*23*). We also noticed radiation-induced lymphopenia, which seemed to be caused by T-cell sequestration to lymph nodes and can be considered a predictor of poor survival in patients with metastatic breast cancer (*30*). Our data also showed neutrophilia for all groups, which can be associated with tumor development and disease outcome (*31*).

Metastasis to vital organs can occur during cancer progression, mainly in advanced stages, and is considered the principal cause of cancer-associated deaths (*9*, *12*). Breast cancer shows metastatic heterogeneity involving the lung, liver, bone, and brain, which leads to varied responses to treatment and patient prognosis (*32*). Indeed, breast cancer cells can spread to distant sites, where they increase rapidly into macroscopic masses (*33*). OCT is a high-resolution technique that has been used in oncology for the early detection of small lesions, which would often not be visible on gross examination, thus increasing the accuracy of the diagnosis (*34*). Our data showed that red light treatment before each dose of radiation, regardless of the light dose, promoted longer and greater survival and reduced the number of metastatic nodules in the lungs.

An imbalance in the antioxidant network by an enhanced formation of reactive oxygen species (ROS) or depletion of antioxidants leads to oxidative stress. Glutathione is an antioxidant found in living cells that fights oxidative stress and plays a dual role in cancer initiation and progression. Indeed, GSH is considered to be one of the most important scavengers of ROS, and its ratio with GSSG can be used as a marker of oxidative stress. GSH's antioxidant role is mostly done by GSH peroxidase (GPx)-catalyzed processes that reduce hydrogen peroxide and lipid peroxide as GSH is oxidized to GSSG. GSSG is then reduced back to GSH at the expense of NADPH by GSSG reductase, forming a redox cycle (*35*).

Our data showed high levels of GSH/GSSG in the tumor and irradiation groups indicating that radiation was ineffective in treating TNBC. This finding supports the claim that enhanced levels of GSH can be linked to treatment resistance, tumor invasiveness, and metastasis (*36*). On the other hand, we noticed that the RL/IR group showed lower GSH/GSSG than the irradiation group. Interestingly, red light treatment can trigger redox modulation after its absorption by photoacceptors in mitochondria (*37*). Mitochondrial GSH is essential for protecting against oxidative stress that is produced both normally and pathologically (*35*). Since more than 10% of the synthesized GSH is found in mitochondria, we hypothesize that the highest dose of red light before each dose of radiation was able to affect the synthesis of the GSH, which rendered tumor cells more

susceptible to red light. Indeed, Lee and collaborators showed that inhibition of GSH synthesis in human TNBC cells promotes a better response to radiation (*38*). Thus, we propose that the inhibition of GSH pathway biosynthesis could increase ROS levels that in turn enhance cell death.

Although PBM is mainly reported to mitigate side effects of radiation, a few studies addressed its radiosensitizing potential (*39–41*). Djavid and coworkers (*39*) showed that PBM at 685 nm and 5 J/cm^2 before exposure to radiation significantly inhibited clonogenic growth of HeLa cells. On the other hand, PBM at 830 nm and 1 J/cm^2 significantly protected fibroblasts against radiation (*39*). Additionally, Tabosa et al. (*40*) investigated the cellular response of oral squamous cell carcinoma exposed to PBM at 660 nm and 300 J/cm^2 before exposure to radiation. The authors concluded that cell growth and clonogenic cell survival were considerably lowered by PBM. Also, PBM groups exhibited a lower rate of migration, a higher rate of cell death and higher intracellular ROS levels than the control group (*40*).

In vivo, Faria et al. (*41*) used PBM (780 nm, 5 J, and 20 mW.cm^{-2}) before irradiation (15 Gy) in xenografic human epidermoid tumors induced in mice. The authors reported a delay in tumor progression and a few regions of necrosis. They assumed that PBM reduced the levels of hypoxia and, consequently, increased the radiation-induced damage.

Curiously, our previous data showed that red light treatment after each dose of radiation promoted significantly better outcomes than radiation alone, regardless of the light protocol (*23*). Here, we noticed that the highest light dose RL/IR significantly arrested tumor progression compared to radiation. Taken together, it seems that red light treatment could be used before or after each dose of radiation, regardless of the light dose, to increase life expectancy and improve the quality of life of patients with TNBC. Further studies are needed to provide scientific evidence of the safe use of PBM associated with radiation exposure.

CONCLUSION

Our findings indicate that red light treatment impacts the effects of radiation. A single red light treatment resulted in similar effects compared to radiation alone but when red light was administered before each dose of radiation, we noticed better outcomes. Both light doses were able to reduce metastases, resulted in better health status, and longer survival of animals. Additionally, the highest light dose was able to radiosensitize TNBC and significantly arrest tumor progression, probably by inhibiting GSH synthesis.

ACKNOWLEDGMENTS

This work was funded by Comissão Nacional de Energia Nuclear, Instituto de Fotônica do Conselho Nacional de Desenvolvimento Científico e Tecnológico (INFO/CNPQ grant: 465763/2014-6) and Sisfóton (grant: 01245.010442/2021-97). The datasets used and analyzed during the current study are available from the corresponding author upon reasonable request.

Received: March 17, 2023; accepted: July 31, 2023; published online: September 13, 2023

REFERENCES

1. Shah C, Bauer-Nilsen K, McNulty RH, Vicini F. Novel radiation therapy approaches for breast cancer treatment. Semin Oncol 2020; 47:209-216.
2. Baskar R, Lee KA, Yeo R, Yeoh K-W. Cancer and radiation therapy: current advances and future directions. Int J Med Sci 2012; 9:193-199.
3. Santivasi WL, Xia F. Ionizing radiation-induced DNA damage, response, and repair. Antioxid Redox Signal 2014; 21:251-259.
4. Baumann M, Krause M, Overgaard J, Debus J, Bentzen SM, Daartz J, et al. Radiation oncology in the era of precision medicine. Nat Rev Cancer 2016; 16:234-249.
5. Yamada Y, Ackerman I, Franssen E, Mackenzie RG, Thomas G. Does the dose fractionation schedule influence local control of adjuvant radiotherapy for early stage breast cancer? Int J Rad Oncol Biol Phys 1999; 44:99-104.
6. Kwan W, Bahl G, Kim D, Ye A, Gagne I, Alexander A. Acute toxicity of ultrahypofractionation compared with moderate hypofractionation in prostate cancer treatment: A randomized trial. Int J Rad Oncol Biol Phys 2022; 113:1036-1043.
7. Meattini I, Becherini C, Boersma L, Kaidar-Person O, Marta GN, Montero A, et al. European Society for Radiotherapy and Oncology Advisory Committee in Radiation Oncology Practice consensus recommendations on patient selection and dose and fractionation for external beam radiotherapy in early breast cancer. Lancet Oncol 2022; 23:21-31.
8. Citrin DE. Recent developments in radiotherapy. N Engl J Med 2017; 377:1065-1075.
9. He L, Lv Y, Song Y, Zhang B. The prognosis comparison of different molecular subtypes of breast tumors after radiotherapy and the intrinsic reasons for their distinct radiosensitivity. Cancer Manag Res 2019; 11:5765-5775.
10. Benjamin D, Smith JRB, Blitzblau R, Freedman G, Haffty B, Hahn C, et al. Radiation therapy for the whole breast: Executive summary of an American Society for Radiation Oncology (ASTRO) evidence-based guideline. Pract Radiat Oncol 2018; 8: 145-152.
11. Gegechkori N, Haines L, Lin JJ. Long-term and latent side effects of specific cancer types. Med Clin North Am 2017; 101: 1053-1073.
12. Al-Mahmood S, Sapiezynski J, Garbuzenko OB, Minko T. Metastatic and triple-negative breast cancer: challenges and treatment options. Drug Deliv Transl Res 2018; 8:1483-1507.
13. Sung H, Ferlay J, Siegel RL, Laversanne M, Soerjamatoram I, Jemal A, et al. Global Cancer Statistics 2020: GLOBOCAN Estimates of incidence and mortality worldwide for 36 cancers in 185 countries. CA Cancer J Clin 2021; 71:209-249.
14. Kumar P, Aggarwal R. An overview of triple-negative breast cancer. Arch Gynecol Obstet 2016; 293:247-269.
15. Yin L, Duan J-J, Bian X-W, Yu S-C. Triple-negative breast cancer molecular subtyping and treatment progress. Breast Cancer Res 2020; 22:61.
16. Ma Y, Zhang H, Chen C, Liu L, Ding T, Wang Y, et al. TRIM32 promotes radioresistance by disrupting TC45-STAT3 interaction in triple-negative breast cancer. Oncogene 2022; 41:1589-1599.
17. Hamblin MR. Mechanisms and applications of the anti-inflammatory effects of photobiomodulation. AIMS Biophys 2017; 4:337-361.
18. Mussttaf RA, Jenkins DFL, Jha AN. Assessing the impact of low level laser therapy (LLLT) on biological systems: a review. Int J Rad Biol 2019; 95:23.

19. Robijns J, Censabella S, Bulens P, Maes A, Mebis J. The use of low-level light therapy in supportive care for patients with breast cancer: review of the literature. Lasers Med Sci 2017; 32:229-242.

20. Baxter GD, Liu L, Petrich S, Gisselman AS, Chapple C, Anders JJ, et al. Low level laser therapy (Photobiomodulation therapy) for breast cancer-related lymphedema: a systematic review. BMC Cancer 2017; 17:833.

21. He MY, Rancoule C, Rehailia-Blanchard A, Espenel S, Trone J-C, Bernichon E, et al. Radiotherapy in triple-negative breast cancer: Current situation and upcoming strategies. Crit Rev Oncol Hematol 2018;131: 96-101.

22. Zahnreich S, Ebersberger A, Karle H, Kaina B, Schmidberger H. Quantification of radiation biomarkers in leukocytes of breast cancer patients treated with different modalities of 3D-CRT or IMRT. Radiat Res 2016; 186: 508-519.

23. Silva CR, Salvego CA, Rostelato ME, Zeituni CA, Ribeiro MS. Photobiomodulation therapy combined with radiotherapy in the treatment of triple-negative breast cancer-bearing mice. J Photochem Photobiol B 2021; 220:9.

24. Silva CR, Pereira ST, Napolitano CM, Somessari ER, Ribeiro MS. Development of a shielding device for radiotherapy of breast cancer-bearing mice. Braz J Rad Sci 2020; 8:1-9.

25. Pereira ST, Silva CR, Nuñez SC, Ribeiro MS. Safety and clinical impact of a single red light irradiation on breast tumor-bearing mice. Photochem Photobiol 2021; 97:435-442.

26. Wang Q, Ye T, Chen H-L, Zhang X-G, Zhang L-Z. Correlation between intensity modulated radiotherapy and bone marrow suppression in breast cancer. Eur Rev Med Pharmacol Sci 2016; 20: 75-81.

27. Wang C, Chen YG, Gao JL, Lyu GY, Su J, Zhang QI, et al. Low local blood perfusion, high white blood cell and high platelet count are associated with primary tumor growth and lung metastasis in a 4T1 mouse breast cancer metastasis model. Oncol Lett 2015; 10:754-760.

28. Shahid S. Review of hematological indices of cancer patients receiving combined chemotherapy & radiotherapy or receiving radiotherapy alone. Crit Rev Oncol Hematol 2016; 105:145-155.

29. Gonzalez H, Hagerling C, Werb Z. Roles of the immune system in cancer: From tumor initiation to metastatic progression. Genes Dev 2018; 32:1267-1284.

30. Chen F, Yu H, Zhang H, Nong Y, Wang Q, Jing H, et al. Risk factors for radiation induced lymphopenia in patients with breast cancer receiving adjuvant radiotherapy. Ann Transl Med 2021; 9: 1288.

31. Shaul ME, Fridlender ZG. Tumour-associated neutrophils in patients with cancer. Nat Rev Clin Oncol 2019; 16:601-620.

32. Liang Y, Zhang H, Song X, Yang Q. Metastatic heterogeneity of breast cancer: Molecular mechanism and potential therapeutic targets. Sem Cancer Biol 2020; 60: 14-27.

33. Jin L, Han B, Siegel E, Cui Y, Giuliano A, Cui X. Breast cancer lung metastasis: Molecular biology and therapeutic implications. Cancer Biol Ther 2018; 19: 858-868.

34. Wang J, Xu Y, Boppart SA. Review of optical coherence tomography in oncology. J Biomed Opt 2017; 22: 1-23.

35. Lu SC. Glutathione synthesis. Biochim Biophys Acta 2013; 1830: 3143–3153.

36. Bansal A, Simon MC. Glutathione metabolism in cancer progression and treatment resistance. J Cell Biol 2018; 217: 2291-2298.

37. Karu TI. Mitochondrial signaling in mammalian cells activated by red and near-IR radiation. Photochem Photobiol 2008; 84: 1091-1099.

38. Lee H, To NB, Kim M, Nguyen T-HY, Cho SK, Choi H-K. Metabolic and lipidomic characterization of radioresistant MDA-MB-231 human breast cancer cells to investigate potential therapeutic targets. J Pharm Biomed Anal 2022; 208:114449.

39. Djavid GE, Goliaie B, Nikoofar A. Analysis of radiomodulatory effect of low-level laser irradiation by clonogenic survival assay. Photomed Laser Surg 2015; 33:452-459.

40. Tabosa ATL, Souza MG, de Jesus SF, Rocha DF, Queiroz LDRP, Santos EM, et al. Effect of low-level light therapy before radiotherapy in oral squamous cell carcinoma: An in vitro study. Lasers Med Sci 2022; 37:3527-3536.

41. Faria CMG, Barrera-Patiño CP, Santana JPP, Avó LRS, Bagnato VS. Tumor radiosensitization by photobiomodulation. J Photochem Photobiol B, Biol 2021; 225:112349.